ISBN: 978-3-95450-208-0 doi:10.18429/JACoW-IPAC2019-MOPMP025

MOVING LONG-RANGE BEAM-BEAM ENCOUNTERS IN HEAVY-ION COLLIDERS

M.A. Jebramcik*[1], J.M. Jowett, CERN, 1211 Geneva 23, Switzerland
[1]also at Goethe University Frankfurt, 60438 Frankfurt am Main, Germany

Abstract

Asymmetric ion beam collisions like proton-lead in the LHC or gold-deuteron in RHIC have become major components of heavy-ion physics programmes. The injection and ramp of two different ion species with the same magnetic rigidity and consequently unequal revolution frequencies generate moving long-range beam-beam encounters in the interaction regions of the collider. These encounters led to fast beam losses and can cause emittance blow-up as observed in RHIC in the early 2000s and, more recently, in 2015. Yet such effects are absent at the LHC so the difference between the two colliders requires explanation.

Tools and models have been developed to describe the beam dynamics of moving long-range beam-beam encounters and to predict the evolution of emittance and other beam parameters. Besides presenting results for RHIC and the LHC we give an outlook for the HL-LHC and potential operational restrictions.

INTRODUCTION

The simultaneous acceleration of two particle types with different charge-to-mass ratios requires special acceleration schemes in heavy-ion colliders like the LHC at CERN and RHIC at Brookhaven National Laboratory (BNL) (see Fig. 1). Assuming that the beams are kept on the central orbits, the two-in-one design of the main bending magnets enforces the same magnetic rigidity $B\rho$ on the two beams during the energy ramp of the LHC. RHIC on the other hand, has the advantage of independent rings of magnets for each beam, allowing acceleration with different rigidities $B\rho$ (within certain limits arising from geometry and the common magnets in the straight sections). Accelerating with the same rigidity causes the two beams to have different velocities at injection and during acceleration and their RF frequencies f_{RF} have to be varied independently. It has been shown [1] that this cannot be avoided with feasible radial displacements of the orbits. This acceleration scheme led to unstable behavior in RHIC during gold-deuteron (Au–D) operations in 2002/2003 [2] and during a test with aluminium-proton (Al–p) in 2015 [3]. The cause was long-range beam-beam encounter positions moving along the interaction regions (IRs) because of the different revolution frequencies, f_0, of the two beams. This led to doubts whether beams of different charge-to-mass ratio could ever be accelerated in the LHC although simple diffusion models and arguments based on the strength of the interactions [1] suggested otherwise. Indeed, there was no sign of such effects during the p–Pb pilot run in 2012 [4], nor in the p–Pb runs in 2013 [5] and 2016 [6],

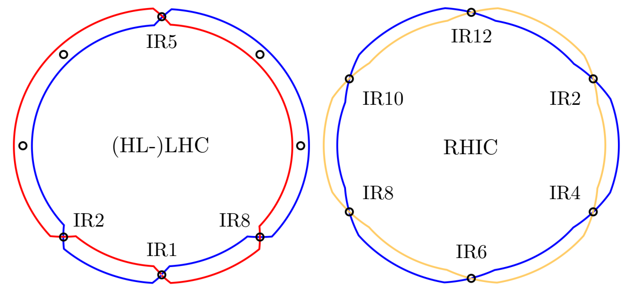

Figure 1: Schematic layout of the LHC (left) and RHIC (right).

which achieved 3–4 orders of magnitude more luminosity. All used equal rigidity injection and acceleration. In this paper we present a more detailed model reproducing the effects in the LHC and RHIC and investigate whether larger bunch numbers and higher bunch intensities may influence the LHC beams in Run 3 and beyond (HL-LHC [7]).

MOVING BEAM-BEAM ENCOUNTERS

Although the beams are typically separated by a few mm at injection, they still interact via long-range beam-beam forces at a number of points all along the interaction regions where they share a common beam pipe. Thanks to the different revolution frequencies, the positions of these long-range beam-beam encounters shift by

$$d_t \approx C \frac{c^2}{4p_\mathrm{p}^2}\left(\frac{m_1^2}{Z_1^2} - \frac{m_2^2}{Z_2^2}\right) \quad (1)$$

per turn. Here, the indices 1, 2 denote the two ion species, C is the circumference, c the speed of light, m the ion mass, Z its atomic number and p_p is the proton momentum at equal rigidity. The long-range beam-beam kick on a particle of the first beam (index 1) is $(\Delta x', \Delta y') \approx (x, y)k/r^2$ with $r^2 = x^2 + y^2$ and $k = 2N_2 r_p m_p Z_1 Z_2/(m_1\gamma_1)$. Here r_p is the classical proton radius, N the bunch intensity, and m_p is the proton mass. The shift d_t and the difference of the two f_{RF} become smaller towards higher energies. At target energy, both f_{RF} are locked to their central frequency enforcing equal frequencies f_0, small radial orbit shifts and momentum shifts $\delta_p \approx \pm\eta d_t/C$ on both beams [1] with η being the slippage factor.

The moving beam-beam encounters cause resonant behavior according to the resonance condition

$$lQ_x + nQ_y = j + q\cdot(2 + Q_v)\,h_\mathrm{b} \quad (2)$$

where $(l, n, j, q) \in \mathbb{Z}^4$, $Q_v = (v_2 - v_1)/v_1$ is an effective "tune" arising from the difference of beam velocities v, and

* marc.jebramcik@cern.ch

ISBN: 978-3-95450-208-0 doi:10.18429/JACoW-IPAC2019-MOPMP025

h_b is the bunch harmonic. These so-called overlap knock-out (OKO) resonances were first observed in the ISR at CERN [8, 9]. The 1st and 2nd order resonances $|l| + |n| = 1$ and $|l| + |n| = 2$ have most effect since higher-order multipole components are relatively small in the far-field. The strength of the 1st order (dipolar) resonances, i.e., the amplitude in frequency space, becomes weaker with larger j. The exact scaling depends on the IR layout, beam separations and phase advance between the IRs.

PSEUDO NON-LINEAR MODEL

Tracking codes based on elements at fixed locations do not lend themselves to the implementation of moving beam-beam encounters with specific bunch filling patterns and bunch-to-bunch intensity variations. A model has been developed to understand this unusual beam dynamics. As a first step, a phase space allowing translation to cover coherent kicks is introduced $\mathbf{r} = (x, x', y, y', 1)^{\mathrm{T}}$ with a 5th scalar vector component. The beam-beam kick can be linearised in matrix form

$$\mathbf{B}(s_i) = \begin{pmatrix} 1 & 0 & 0 & 0 & 0 \\ \frac{\partial \Delta x'(d_x,d_y)}{\partial x} & 1 & \frac{\partial \Delta x'(d_x,d_y)}{\partial y} & 0 & \Delta x'(d_x, d_y) \\ 0 & 0 & 1 & 0 & 0 \\ \frac{\partial \Delta y'(d_x,d_y)}{\partial x} & 0 & \frac{\partial \Delta y'(d_x,d_y)}{\partial y} & 1 & \Delta y'(d_x, d_y) \\ 0 & 0 & 0 & 0 & 1 \end{pmatrix}. \tag{3}$$

Here, d_u (u either x or y) is the separation between the centroid of the test and opposing beam at an encounter position s_i and the derivatives of the beam-beam kick are evaluated at $(x, y) = (d_x, d_y)$. The transfer matrix *for a particular turn of the ring* $\mathbf{T} = \prod_{i=1}^{N} \mathbf{R}(s_{i+1}, s_i)\mathbf{B}(s_i)$ is obtained by alternately multiplying beam-beam matrices $\mathbf{B}$ and linear transfer matrices

$$\mathbf{R}(s_{i+1}, s_i) = \mathrm{diag}\left(\mathbf{R}_x(s_{i+1}, s_i),\ \mathbf{R}_y(s_{i+1}, s_i),\ 1\right) \tag{4}$$

with $\mathbf{R}_u$ being the standard 2×2 linear transfer matrix. This model lacks effects like amplitude detuning as well as tune oscillation from chromaticity in combination with synchrotron motion. To cover these effects, a turn of the ring is split up in different parts. In the IRs, the nominal tune is assumed for all particles and therefore the linear transfer matrix representing the respective IR, $\mathbf{M}_{\mathrm{IR}}$, comprising the beam-beam interactions, is the same for all particles. In the arcs, the phase advance of the transfer matrices $\mathbf{R}_{\mathrm{arc}}$ (see Eq. (4)) is modified as follows. The tune deviation of a particle during a turn is approximated with

$$\Delta Q_u \approx \alpha_{ux} J_x + \alpha_{uy} J_y + \xi_u \frac{\Delta p}{p_0} \sin(2\pi Q_s n + \varphi_0)\,. \tag{5}$$

Here, α_{ij} are the linear detuning parameters with $\alpha_{xy} = \alpha_{yx}$, J_u are linear action variables, ξ_u is the chromaticity, $\Delta p/p_0$ is the relative momentum error, Q_s is the synchrotron tune, n is the turn number and φ_0 is an arbitrary phase. The tune shift in Eq. (5) is distributed according to the linear phase advance in the arcs, i.e., $\mathrm{d}\Delta Q_u(s)/\mathrm{d}s \propto 1/\beta_u(s)$. Tracking is performed by multiplying IR matrices $\mathbf{M}_{\mathrm{IR}}$ and arc matrices $\mathbf{R}_{\mathrm{arc}}$ containing modified particle-specific phase advances which are constantly updated. The higher order-multipole components of the moving beam-beam interactions are weak at large betatron amplitudes where lattice non-linearities may limit dynamic aperture. Since the dynamic aperture is normally ample at injection, we can neglect these effects in our model. The model also assumes the counter-rotating beam to be *strong*, i.e., rigid and undisturbed.

Table 1: Key Parameters at Injection Energy for the LHC's 2016 p–Pb Run and RHIC's 2002/2003 Au–D Run

	LHC (Pb, p)	RHIC (Au, D)
Inj. energy E_0 (Z GeV)	450	24.4
Circumference C (m)	26658.88	3833.85
Rel. Lorentz factor γ	(191, 480)	(10.52, 13.00)
Horizontal tune Q_x	64.28	28.277
Vertical tune Q_y	59.31	29.287
Norm. emit. ϵ_n (µm)	(2.0, 2.5)	(2.2, 2.2)
Part. per bunch N (10^8)	(2.1, 280)	(7, 1200)
Shift per turn d_t (m)	0.15	3.01
OKO tune Q_v (10^{-3})	0.01	1.57

THE LHC, HL-LHC AND RHIC

The model has been used to study the emittance evolution of a *weak* Pb bunch in Beam 1 of the LHC and of an Au bunch in the Blue ring in RHIC, both at injection energy where the encounter shift d_t is largest, beam rigidities are smallest and effects should be worst.

Layouts and parameters of LHC and RHIC are given in Fig. 1 and Table 1. The Lorentz factor γ in the LHC is more than one order larger than in RHIC. At RHIC's injection energy, equivalent to $B\rho = 81$ T m [10], the tune Q_v is much larger than in the LHC. The required j for dipolar resonances to approach RHIC's transverse betatron tunes is in the $j \approx 4 \times 10^2$ range while it is two orders larger in the LHC with $j \approx 5 \times 10^4$ assuming $h_b = 1$. Another key difference is the layout with the LHC having four and RHIC six IRs. The beam-pipe crotch distance in the LHC is at least 225 m comprising roughly 16 beam-beam encounters with a 100 ns proton bunch spacing as in 2016. In RHIC, the beam-pipe crotches are 32 m apart and only two encounters can occur with a filling of 110 bunches. In the LHC, the beam separations are either ±2 mm (IR1/5) or ±3.5 mm (IR2/8) in horizontal (IR1/2) and vertical (IR5/8) plane. In RHIC, the separations are ±5 mm in the vertical plane. Besides the Pb–p runs up to 2016, the future "HL-LHC" operation has also been analysed. The differences from the 2016 LHC in Pb–p operations at injection are marginal. Key differences are betatron tunes of $(Q_x, Q_y) = (62.27, 60.295)$ in use since 2018, and slightly shorter common beam pipes in IP1/5.

The kicks applied to the weak beam depend on the filling pattern of the counter-rotating beam. The patterns are affected by the RF manipulations, rise times of injection and ex-

ISBN: 978-3-95450-208-0 doi:10.18429/JACoW-IPAC2019-MOPMP025

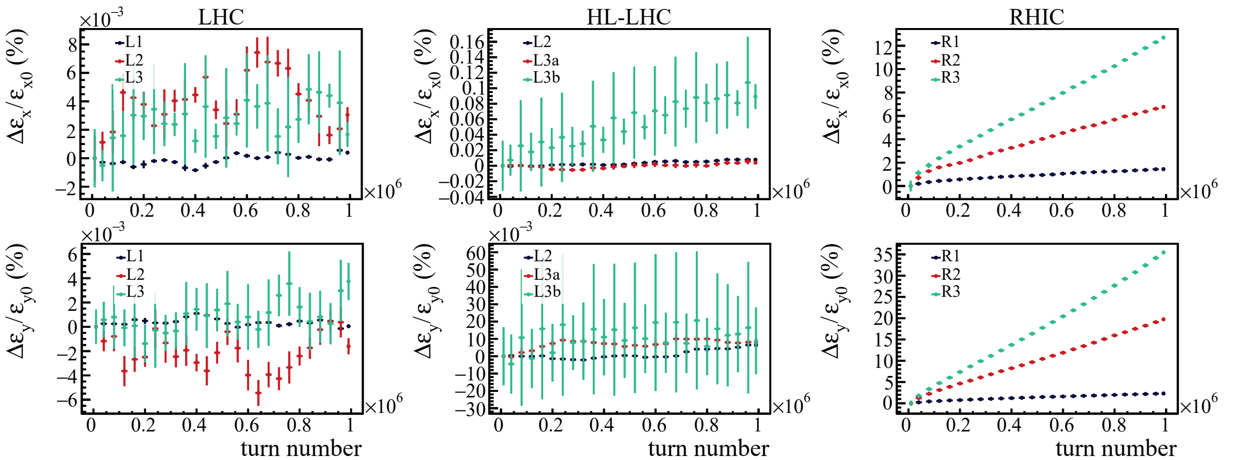

Figure 2: Relative horizontal (top) and vertical (bottom) emittance change vs. turn number for a Pb bunch in the LHC (left), HL-LHC (centre) and for a Au bunch in RHIC (right) for three different filling patterns.

traction kickers and other properties of the colliders and their respective injector chains. Bunch spacing and unevenness along the bunch train influence the kick spectrum and therefore three different filling patterns were simulated for each collider (Table 2). For the LHC, a bunch pattern with only 15 bunches (L1), a pattern with 684 bunches from 2016 (L2) and an HL-LHC filling pattern with 1232 bunches (L3) [11] were treated. For the HL-LHC, a bunch pattern with 684 bunches (L2) was analysed as well as the nominal 1232 bunches with two proton bunch intensities $N_{b2} = 2.8 \times 10^{10}$ (L3a), which is typical for Pb–p operation, and 1.15×10^{11} (L3b), a much higher value typical of p–p operation. For RHIC, patterns with $k_{b2} = 1$ (R1), 55 (R2) and 110 deuteron bunches (R3) were simulated.

SIMULATION RESULTS

The emittance evolution for a Pb bunch in the LHC/HL-LHC and for a Au bunch in RHIC are given in Fig. 2 and

Table 2: List of filling patterns for the LHC, HL-LHC and RHIC. The number of proton/deuteron bunches, k_{b2}, bunch populations, N_{b2} and fitted linear growth rates normalised to the initial emittance ($\dot{\varepsilon}_u/\varepsilon_{u0}$) of the Pb/Au beams are given.

Filling pattern	k_{b2}	N_{b2} (10^{10})	$\dot{\varepsilon}_x/\varepsilon_{x0}$ (10^{-5}/s)	$\dot{\varepsilon}_y/\varepsilon_{y0}$ (10^{-5}/s)
			LHC	
L1	15	2.8	0.01 ± 0.00	< 0.01
L2	684	2.8	0.02 ± 0.01	< 0.01
L3	1232	2.8	0.03 ± 0.01	0.03 ± 0.01
			HL-LHC	
L2	684	2.8	0.10 ± 0.01	0.08 ± 0.01
L3a	1232	2.8	0.07 ± 0.02	0.07 ± 0.02
L3b	1232	11.5	1.05 ± 0.06	0.11 ± 0.04
			RHIC	
R1	1	12	100 ± 4	166 ± 5
R2	55	12	495 ± 9	1503 ± 11
R3	110	12	940 ± 11	2718 ± 22

fitted linear growth rates are listed in Table 2. The error bars in Fig. 2 are the standard deviation arising from applying a moving average. None of the three filling patterns created any obvious emittance increase in the nominal LHC. Even the pattern with $k_{b2} = 1232$ bunches (L3) barely influences the emittances. The HL-LHC displays the same stability for the filling patterns L2 and L3a. The HL-LHC pattern with high p intensities (L3b) generates emittance increase of 0.1 % over 10^6 turns (~89 s), which is insignificant considering the presence of radiation damping, intra-beam scattering and a transverse feedback system. The Au bunch in RHIC experiences major emittance blow-up in all cases. Over 10^6 turns (~13 s), the emittance increases by roughly 13 % in the horizontal and 36 % in the vertical plane with 110 bunches which is consistent with observations [10] and leads to unacceptable intensity loss.

CONCLUSION

The model reproduces the observed behaviour of the LHC: beams are stable and barely influenced by moving encounter points. In future, the HL-LHC can be expected to be stable even with unrealistically high proton bunch intensities. The model also shows that RHIC was inoperable with unequal revolution frequencies, as observed in 2002/2003. The smaller injection energy and therefore much larger tune Q_v, the lower rigidity and larger net beam-beam kicks lead to a stronger excitation of the beams compared to the LHC. For this reason, RHIC has been operated with equal revolution frequencies since 2003. As a next step, the 2015 Al–p test with unequal frequencies will be analysed to see if the observed intensity decays are reproduced.

ACKNOWLEDGEMENTS

We thank W. Fischer, S. Tepikian and R. Versteegen for very helpful discussions and information. This work has been sponsored by the Wolfgang Gentner Programme of the German Federal Ministry of Education and Research (grant no. 05E15CHA).

ISBN: 978-3-95450-208-0 doi:10.18429/JACoW-IPAC2019-MOPMP025

REFERENCES

[1] J. M. Jowett and C. Carli, "The LHC as a Proton-nucleus Collider", in *Proc. 10th European Particle Accelerator Conf. (EPAC'06)*, Edinburgh, UK, Jun. 2006, paper MOPLS009, pp. 550–552.

[2] T. Satogata *et al.*, "Commissioning of RHIC Deuteron-Gold Collisions", in *Proc. 20th Particle Accelerator Conf. (PAC'03)*, Portland, OR, USA, May 2003, paper TPPB043, pp. 1706–1708.

[3] C. Liu *et al.*, "Attempt to accelerate asymmetric species with unequal frequencies in RHIC", Brookhaven National Laboratory, Upton, USA, Rep. BNL-108493-2015-IR, July 2015. https://www.bnl.gov/isd/documents/89396.pdf

[4] R. Alemany Fernandez *et al.*, "First proton-nucleus collisions in the LHC: the p-Pb pilot physics", CERN, Geneva, Switzerland, Rep. CERN-ATS-Note-2012-094 MD, November 2012. https://cds.cern.ch/record/1496101

[5] J. M. Jowett *et al.*, "Proton-nucleus Collisions in the LHC", in *Proc. 4th Int. Particle Accelerator Conf. (IPAC'13)*, Shanghai, China, May 2013, paper MOODB201, pp. 49–51. http://cds.cern.ch/record/1572994

[6] J. M. Jowett *et al.*, "The 2016 Proton-Nucleus Run of the LHC", in *Proc. 8th Int. Particle Accelerator Conf. (IPAC'17)*, Copenhagen, Denmark, May 2017, pp. 2071–2074. doi:10.18429/JACoW-IPAC2017-TUPVA014

[7] G. Apollinari *et al.*, editors, "High-Luminosity Large Hadron Collider (HL-LHC) : Technical Design Report V. 0.1", CERN, Geneva, Switzerland, Rep. CERN-2017-007-M, 2017. https://cds.cern.ch/record/2284929

[8] J. P. Gourber, H. G. Hereward and S. Myers, "Overlap Knock-Out Effects in the CERN Intersecting Storage Rings (ISR)", *IEEE Transactions on Nuclear Science*, vol. 24, pp. 1405-1407, 1977. doi:10.1109/TNS.1977.4328959

[9] S. Myers, "Overlap knock-out resonances with colliding bunched beams in the CERN ISR", *IEEE Transactions on Nuclear Science*, vol. 26, pp. 3574-3576, 1979. doi:10.1109/TNS.1979.4330104

[10] W. Fischer, "RHIC with asymmetric ion beams", Seminar on feasibility of p-Pb in the LHC, Geneva, Switzerland, 2011.

[11] J. M. Jowett *et al.*, LHC Performance Workshop, Chamonix, France, 2017. https://indico.cern.ch/event/580313/